PCSS Hand: An Underactuated Robotic Hand with a Novel Parallel-Coupled Switchable Self-adaptive Grasp

Shuang Song and Wenzeng Zhang(✉)

Department of Mechanical Engineering,
Tsinghua University, Beijing 100084, China
wenzeng@tsinghua.edu.cn

Abstract. This paper proposes a novel concept of underactuated grasping mode, called PCSS grasping mode. This mode has switchable hybrid grasping functions: parallel self-adaptive grasping (PASA) and coupled self-adaptive grasping (COSA), being able to grasp larger range of objects with different shapes and dimensions than traditional PASA and COSA hands. The PCSS grasping can execute different grasping modes: a parallel pinching (PA); a coupled hooking (CO); a self-adaptive encompassing (SA); parallel and self-adaptive hybrid grasping (PASA); coupled and self-adaptive hybrid grasping (COSA). A PCSS Hand is developed with three PCSS fingers and 6 degrees of freedom. Simulation analysis shows the high stability and the versatility of the PCSS Hand.

Keywords: Robotic hand · Underactuated finger · Grasping mode · Self-adaptive grasp · Coupled grasp

1 Introduction

Robotic hands are designed to accomplish different tasks as a capable end-effector of industrial and service robots. Similar to human hands, robotic hands are expected to be capable of grasping large range of objects with different shapes and dimensions. Reproducing the numerous advantages of human hand by mechanism devices is always the ultimate pursuit of the scientific exploration of intelligent robot hands.

Human hands are dexterous and stable, having 21 degrees of freedom, huge power, quick actions while small volume. A common human hand can grasp plenty of different objects because it can perform multiple grasping modes (or grasping configuration).

The research of multi-fingered robotic hand is mainly divided into two kinds: (1) Dexterous hands and (2) Underactuated hands.

Dexterous hands are robotic hands with many degrees of freedom (DOFs) and driven by many actuators. Robotic hands of this type are able to perform different gestures like human hands. The UTAH/MIT Hand [1], Salisbury Hand [2] are outstanding examples of the first generation of dexterous robotic hands. In the recent few years, multiple dexterous hands, such as MANUS Hand [3], High-speed Multi-fingered Hand [4], HIT/DLR Hand [5], Gifu Hand [6] are researched and developed. But

A. Agah et al. (Eds.): ICSR 2016, LNAI 9979, pp. 481–491, 2016.
DOI: 10.1007/978-3-319-47437-3_47

dexterous hands still have defects of complex controlling system and expensive manufacturing costs due to the multiple actuators applied.

In 1970s, underactuated hands are developed to solve these problems. In the area of robotic hand, underactuation is defined as the number of the actuators is smaller than the number of joint degrees of freedom (DOFs). There are many underactuated hands developed, such as: SARAH Hand [7–9] by Laval Univ., SDM Hand [10], and LARM Hand [11]. Different underactuated hands are designed to meet different needs in industrial applications.

Traditional underactuated hands have only one grasping mode, which limits the grasping ability when applied in robots. This paper proposes a novel underactuated grasping concept, called Parallel-Coupled Switchable Self-adaptive (PCSS in short) grasping, which integrates all the five existing underactuated grasping modes and allows underactuated hands to grasp a larger range of objects than former ones. The concept and theory of PCSS grasp is introduced in detail in the second part of this paper; the third part shows the design of PCSS Hands; the forth part analyzes the kinematic and kinetic issues of the PCSS Hands.

2 Concept and Theory of the PCSS Grasping

2.1 Concept of the PCSS Grasping

As mentioned in the former part, an underactuated robotic hand with two phalanges has three basic grasping modes and two hybrid grasping modes (as shown in Fig. 1):

(1) Parallel pinching (PA). In this grasping mode, the distal phalanx of the hand keeps parallel to its original orientation during its movement.
(2) Coupled hooking (CO). In this grasping mode, when the proximal phalanx turns forward relative to the base, the distal phalanx simultaneously turns forward relative to the proximal phalanx.

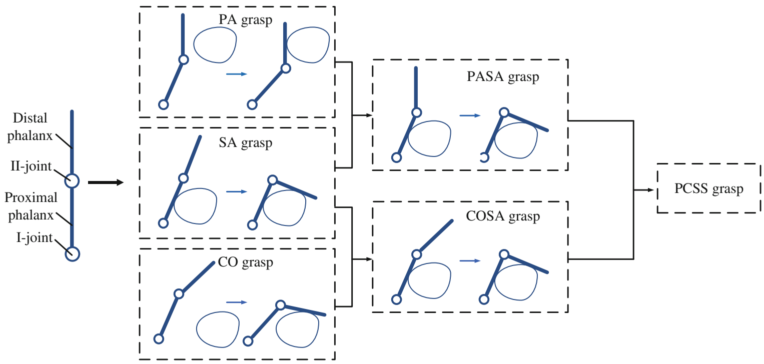

Fig. 1. Underactuated grasping modes.

(3) Self-adaptive encompassing (SA). In this grasping mode, that the final gesture of the finger is determined by the size and shape of the object grasped. The distal phalanx of the SA finger moves after the proximal phalanx blocked by the object.
(4) Parallel and self-adaptive grasping (PASA). The PASA hybrid grasping mode is a combination of the PA grasping mode and the SA grasping mode. In this mode, the finger moves in a PA pattern at the start, if the distal phalanx is blocked by the object, the finger perform a parallel pinching; if the proximal phalanx is blocked by the object, the distal phalanx continues to rotate until touch the object and perform a self-adaptive encompassing.
(5) Coupled and self-adaptive grasping (COSA). The COSA hybrid grasping mode is a combination of the CO grasping mode and the SA grasping mode. Similar to the PASA finger, the COSA finger can perform coupled hooking and self-adaptive encompassing.

The hybridism of basic grasping modes allows underactuated fingers to grasp larger range of objects, but the PASA mode and the COSA mode are not the end of this. These two hybrid grasping modes still have defects: the PASA grasping mode cannot hook; the COSA grasping mode cannot pinch. As each of the three basic grasping modes (CO, PA and SA) can grasp specific kinds of objects which other basic grasping modes cannot perform, further combination will bring further advantages. This paper proposes a higher level combination of the COSA grasping mode and the PASA grasping mode (as shown in Fig. 1), called PCSS grasping mode, which will allow robotic hands to perform almost all the grasping gestures needed in daily applications (Table 1).

Table 1. Performances of underactuated fingers.

Objects	CO	PA	SA	COSA	PASA	PCSS
Ball	No	No	Yes	Yes	Yes	Yes
Cylinder	No	No	Yes	Yes	Yes	Yes
Coin	No	Yes	No	No	Yes	Yes
Bar	Yes	No	No	Yes	No	Yes
Handle	Yes	No	No	Yes	No	Yes
Cube	No	Yes	No	No	Yes	Yes
Irregular	No	No	Yes	Yes	Yes	Yes

2.2 Theory of the PCSS Grasping

In PCSS grasping, the combination of the PASA mode and the COSA mode is achieved by switching between these two modes, which allows underactuated hands to perform both of these two modes while does not need complex switch manipulation. The PCSS hand can perform PASA and the COSA grasping as a result of the cooperation of the limitation part and the driving part.

The limitation part allows the PCSS finger to move in the PA and the CO pattern and to switch between the two modes. The switching between the PA mode and the CO mode is equivalent to the changing of the structure between a parallelogram structure and a crossed “8” structure. In order to achieve this by simple manipulation, this paper proposes a switch method based on open-loop pulley-tendon mechanism, including a half pulley, an open-loop tendon, an entire pulley, a tensioning spring, a switch shaft. The transmission ratio between the two pulleys is 1, assuring the parallel transmission while in the PA mode. The two ends of the open-loop tendon are fixed on the two pulleys in the pattern shown in Fig. 2. The tensioning spring is set on the other side of the pulley-II to make the tendon keep tight. The switch shaft is fixed on the base, set vertical to the I-joint shaft. The half-pulley can roll over across the switch shaft, and this is its only degree of freedom.

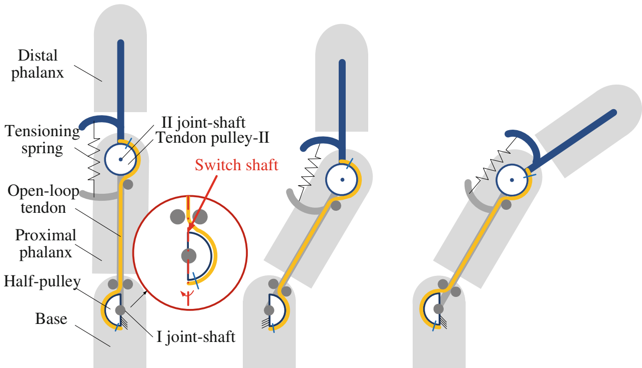

Fig. 2. The switching method of the PCSS grasping mode.

When the half pulley is on the right side (in the view of Fig. 2), the pulley-tendon mechanism is in parallel structure; and on the left side, crossed structure. This switch manipulation can be easily achieved by an actuator applied on the switch shaft or a simple two-position switch applied on the half-pulley.

The driving part allows the PCSS finger to perform the PASA and COSA modes. The hybrid grasping modes have two steps of motion. Take the PASA mode as an example, in the first step the proximal phalanx is driven to rotate across the I-joint shaft while the distal phalanx keeps parallel to its original orientation; and in the second step the proximal phalanx is blocked by the object and the distal phalanx is driven to rotate across the II-joint shaft until touching the object. The driven parts of these two steps are different. The main function of the driving part is to actuate the proximal phalanx at the first step and the distal phalanx at the second step. A pulley-belt transmission mechanism serves as the driving part of the PCSS Hand (as shown in Fig. 3(a)).

The active pulley is set on the I-joint shaft and the passive pulley is fixed on the II-joint shaft. The transmission ratio between the two belt pulleys defines as i. The distal phalanx and the tendon pulley-II are also fixed on the II-joint shaft. The driving part has two DOFs when the active pulley is driven: the rotation of the proximal phalanx relative to the base and the rotation of the distal phalanx relative to the proximal phalanx. The rotation of the proximal phalanx has the priority because of the

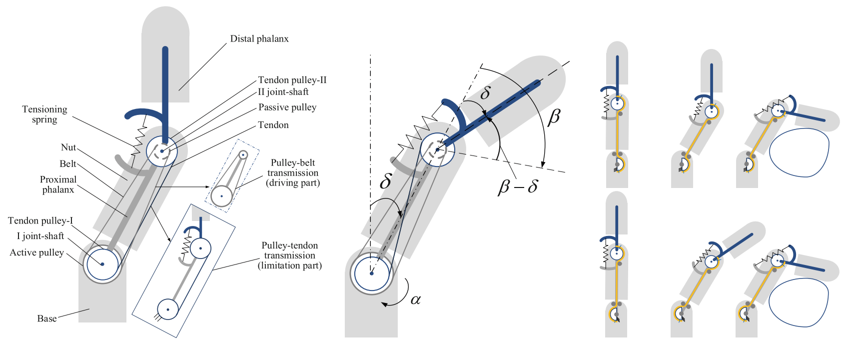

(a) The mechanism structure. (b) Geometric analysis. (c) The PASA and COSA grasp.

Fig. 3. The mechanism structure and function of the PCSS Hand.

tensioning spring. During the rotation of the proximal phalanx, the tensioning spring keeps pulling the tendon, keeping the distal phalanx to match the PA (and CO) grasping mode.

The relationship of the rotation angles of this step is determined by the transmission ratio i. To analyze angle relationship, one can see the motion of the PCSS finger in divided procedures. In the COSA mode, as shown in Fig. 3(b), the motion can be illustrated by: the distal phalanx rotate forward β relative to the proximal phalanx, the proximal phalanx rotates δ relative to the ground and the distal phalanx rotates backward an $\beta - \delta$ relative to the proximal phalanx. The adding result of these procedures is that the angle between the distal phalanx and the extension line of the proximal phalanx equals to δ, which correspond with the feature of the CO grasping mode.

$$\beta = \alpha/i \tag{1}$$

$$\beta - \delta = \delta/i \tag{2}$$

The consociation of Eqs. (1) and (2) makes:

$$\alpha = (i + 1)\delta \tag{3}$$

Similarly, the equation of the PASA mode is:

$$\alpha = (i - 1)\delta \tag{4}$$

When comes to the second step of the hybrid grasping modes, the proximal phalanx is blocked by the object. If the actuator continues to drive the active pulley, the passive pulley along with the distal phalanx will be driven to rotate relative to the proximal phalanx against the force of the tensioning spring. The PASA and COSA function of the PCSS finger and the conditions of the tensioning spring is shown in Fig. 3(c).

It the second step, the tendon will become loose as the distal phalanx rotate forward to execute a self-adaptive encompassing. Additional contemporary tendon storage device is needed to keep the tendon on its track. Small light spring or brand can serve as this device (not shown in Fig. 3).

3 Design of the PCSS Hand

Based on the PCSS grasping concept and its basic theory, a PCSS Hand is designed in detail in this paper. The design of the PCSS Hand with three fingers is shown if Fig. 4.

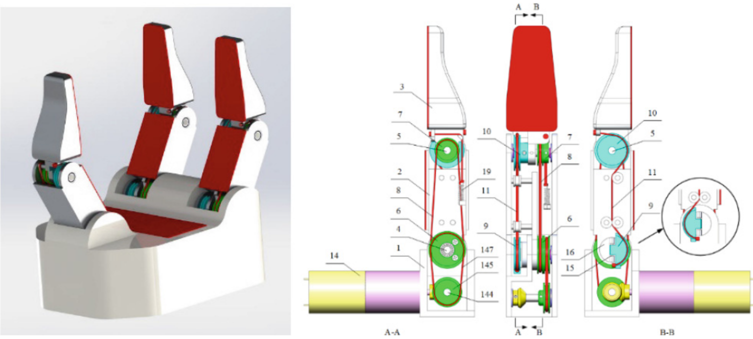

Fig. 4. The design of the PCSS Hand.

Items marked in Fig. 4:

1 - Base; 2 - Proximal phalanx; 3 - Distal phalanx; 4 - I-joint shaft; 5 - II-joint shaft; 6 - Active pulley; 7 - Passive pulley; 8 - Belt; 9 - Tendon pulley-I; 10 - Tendon pulley-II; 11 - Tendon; 14 - Actuator; 15 - Connector; 16 - Switch shaft; 17 - Tensioning Spring.

As mentioned in the former part, the switch function can be also achieved by the rotation of the tendon pulley-I, the prototype is made under this theory to prove the capability of the finger to execute the PASA and the COSA grasping mode. The small spring used to tension the tendon while SA grasping is applied on this prototype.

4 Kinematic Simulation and Kinect Analysis

The PCSS Hands can grasp a large variety of objects because of its multiple grasping modes. To evaluate and optimize the performance of the PCSS Hand, numerical analysis is needed. In this part, the kinematic simulation is carried out to obtain the stable grasping area; Kinect analysis is carried out to calculate the contact force distribution of the hand to evaluate the grasp ability. The PCSS Hand is selected for numerical and experimental evaluation.

4.1 Kinematic Simulation of the PCSS Hand

For the PCSS underactuated hand, the grasp orientation is determined by the size and shape of the object. Once the position and dimension of the object and the basic parameters of the hand are given, the orientation of the hand is predictable.

A simplified kinematic diagram of the PCSS Hand is shown in Fig. 5. The variables $\theta_{1,r}, \theta_{2,r}, \theta_{1,l}, \theta_{2,l}$ represents the rotation angles of the proximal and the distal phalanges of the right and the left finger. The center position of the object is (X_{obj}, Y_{obj}) in the local frame, and the radius of the object is r_{obj}. h_1 and h_2 represents the distance between the contact point on the proximal to the I-joint and distance between the contact point on the distal phalanx to the II-joint.

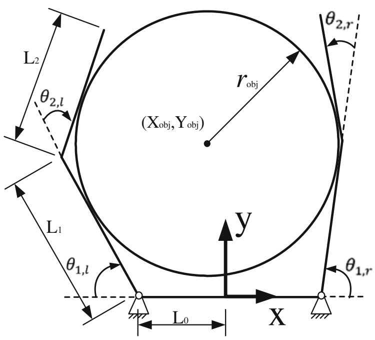

Fig. 5. Kinematic model of the PCSS Hand.

Take the right finger as the subject. According to two different geometric loop closure vectors, the relationship between the parameters above is arrived at the following equations:

$$\begin{pmatrix} L_0 \\ 0 \end{pmatrix} + \mathbf{R}_{\theta_1} \begin{pmatrix} h_1 \\ 0 \end{pmatrix} = \begin{pmatrix} X_{obj} \\ Y_{obj} \end{pmatrix} - \mathbf{R}_{\theta_1} \begin{pmatrix} 0 \\ r_{obj} \end{pmatrix} \tag{5}$$

$$\begin{pmatrix} L_0 \\ 0 \end{pmatrix} + \mathbf{R}_{\theta_1} \begin{pmatrix} L_1 \\ 0 \end{pmatrix} + \mathbf{R}_{\theta_1}\mathbf{R}_{\theta_2} \begin{pmatrix} h_2 \\ 0 \end{pmatrix} = \begin{pmatrix} X_{obj} \\ Y_{obj} \end{pmatrix} - \mathbf{R}_{\theta_1}\mathbf{R}_{\theta_2} \begin{pmatrix} 0 \\ r_{obj} \end{pmatrix} \tag{6}$$

$\mathbf{R}_\theta$ is the rotation matrix:

$$\begin{bmatrix} \cos\theta & -\sin\theta \\ \sin\theta & \cos\theta \end{bmatrix} \tag{7}$$

Simplify Eqs. (5) and (6), one achieves:

$$\theta_1 = \arctan\left(\frac{X_{obj} - L_0}{-Y_{obj}}\right) + \arctan\left(\frac{r_{obj}}{\sqrt{Y_{obj}^2 + \left(X_{obj}^2 - L_0^2\right)}}\right) \tag{8}$$

$$\theta_2 = \pi - 2\arctan\left(\frac{r_{obj}}{L_1 - \sqrt{Y_{obj}^2 + \left(X_{obj}^2 - L_0^2\right) - r_{obj}^2}}\right) \tag{9}$$

From Eqs. (8) and (9), one can study the relationship between the position of the object and the final gesture of the PCSS Hand in the SA mode. As shown in Fig. 6, the rotation angle has limitation caused by the mechanism structure, $60^\circ \leq \theta_1 \leq 135^\circ$, $-30^\circ \leq \theta_2 \leq 90^\circ$. Simulation results show that the PCSS Hand has a large stable grasping area.

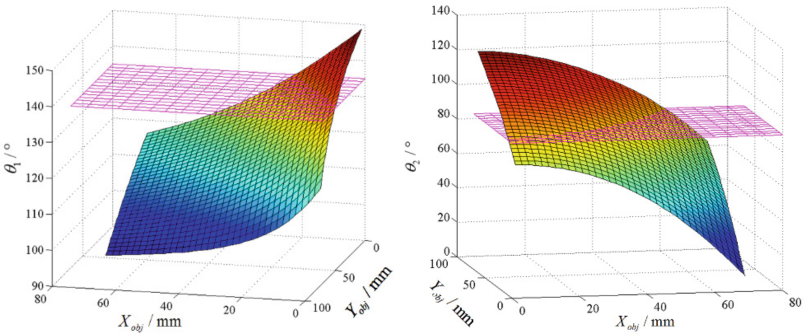

(a) Relationship between $\theta_1$and (X_{obj}, Y_{obj}). **(b)** Relationship betweenθ_2 and (X_{obj}, Y_{obj}).

Fig. 6. Kinematic simulation of the PCSS hand.

Similarly, the equivalent of the rotation angles according to the position of the object if the final orientation of the PCSS Hand is in PA or CO mode can also be achieved by geometric relationship:

If the final orientation of the hand is in PA mode,

$$\theta_2 = -\theta_1 \tag{10}$$

$$\theta_1 = \arccos\left(\frac{r_{obj} + X_{obj} - L_0}{L_1}\right) \tag{11}$$

If the final orientation of the hand is in PA mode,

$$\theta_2 = \theta_1 \tag{12}$$

$$r_{obj} = \left(X_{obj} - 2L_0\right)\sin 2\theta_1 - Y_{obj}cos2\theta_1 - L_1 \sin\theta_1 \tag{13}$$

By the method of kinematic simulation, the grasping area of the PCSS Hand can be achieved, which serves as an important parameter of the ability and stability of the hand. According to the results of the kinematic simulation, the evaluation and optimization of the design is achieved. Furthermore, the kinematic simulation is also a functional method for intelligence robotic hands to estimate the capability of grasping a detected object before the grasping conduct as only the dimension and position of the object are need when calculating the rotation angles.

4.2 Grasping Force Analysis of the PCSS Hand

This part analysis the force distribution of the PCSS Hand. For the reason of simplification, the gravity and the friction are neglected and the contact force are applied on points. Figure 7 shows the dynamical condition of a PCSS finger. The driving torque of the actuator denotes T_M, the torque produced by the spring denotes T_s, F_1 and F_2 are the contact force of the object, f is the tension force in the belt. The transmission ratio of the pulley-belt mechanism denotes a.

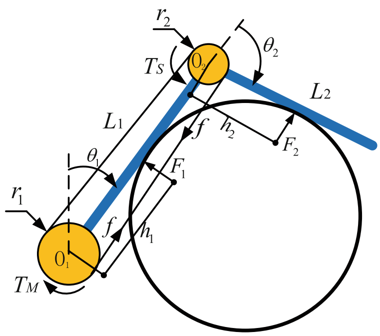

Fig. 7. Grasping force distribution of the PCSS finger.

$$T_M = F_1 h_1 + F_2(h_2 + L_1\cos\theta_2) \tag{14}$$

$$T_M = fr_1 \tag{15}$$

$$T_s + fr_2 = F_2 h_2 \tag{16}$$

Form Eqs. (14)–(16), one obtains the expression equivalent of F_1 and F_2.

$$F_1 = \frac{T_M}{h_1}\left(1 - \frac{h_2 + L_1\cos\theta_2}{ah_2}\right) + \frac{T_s(h_2 + L_1\cos\theta_2)}{h_1 h_2} \tag{17}$$

$$F_2 = \frac{T_M}{ah_2} + \frac{T_s}{h_2} \tag{18}$$

The relationship between the contact force and the contact point on the phalanxes is studied as shown in Fig. 8.

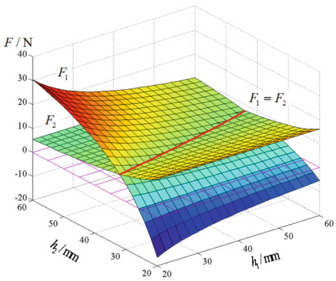

(a) $\theta_1 = 60°, \theta_2 = 30°$

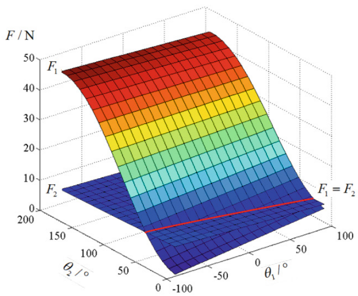

(b) $h_1 = 40\text{mm}, h_2 = 40\text{mm}$

Fig. 8. Contact force distribution by h_1 and h_2 when $T_M = 1400\text{N}\cdot\text{mm}, T_s = 200\text{N}\cdot\text{mm}$, $L_1 = 100\,\text{mm}, a = 16/7$

5 Conclusion

This paper proposes PCSS underactuated grasp mode, which has switchable hybrid grasping modes: parallel self-adaptive grasping mode (PASA) and coupled self-adaptive grasping mode (COSA). The theory of the PASA and COSA structure and the switch function is illustrated in detail. This paper proposes the design of the novel PCSS Hands to prove the theory of PCSS grasping. A PCSS Hand is developed with three PCSS fingers and 6 degrees of freedom (DOFs). The PCSS finger has two joints, mainly consists of an actuator, an accelerative pulley-belt mechanism, an open-looped tendon mechanism, a spring, and a switching mechanism. A prototype based on the theory in manufactured. Kinematic simulation and kinetic analysis are included in this paper indicating the stability and capability of the PCSS Hand. Experimental results show the high the versatility of the PCSS Hand.

Acknowledgement. This paper was supported by the Natural Science Foundation of China (No. 51575302).

References

1. Jacobsen, S.C., Iversen, E.K., Knutti, D.F., et al.: Design of the UTAH/M.I.T. dextrous hand. In: IEEE International Conference on Robotics and Automation, San Francisco, USA, April, pp. 1520–1532 (1986)
2. Salisbury, J.K., Craig, J.J.: Articulated hands: force control and kinematic issues. Int. J. Robot. Res. **1**(4), 4–17 (1982)
3. Pons, J.L., Rocon, E., Ceres, R., et al.: The MANUS-hand dexterous robotics upper limb prosthesis: mechanical and manipulation aspects. Auton. Robots. **16**, 143–163 (2004)
4. Mizusawa, S., Namiki, A., Ishikawa, M.: Tweezers type tool manipulation by a multifingered hand using a high-speed visual servoing. In: 2008 IEEE/RSJ International Conference on Intelligent Robots and Systems. Nice, France. pp. 2709–2714 (2008)
5. Liu, H., Meusel, P., Hirzinger, G., et al.: The modular multisensory DLR-HIT-Hand: hardware and software architecture. Trans. Mechatornics **13**(4), 461–469 (2008)
6. Mouri, T., Kawasaki, H., Yoshikawa, K., et al.: Anthropomorphic robot hand: Gifu Hand III. In: International Conference on Control, Automation and Systems (ICCAS). Jeonbuk, Korea, pp. 1288–1293 (2002)
7. Laliberte, T., Gosselin, C.M.: Simulation and design of under-actuated mechanical hands. Mech. Mach. Theory **33**(1/2), 39–57 (1998)
8. Birglen, L., Gosselin, C.M.: Kinetostatic analysis of underactuated fingers. IEEE Trans. Robot. Autom. **20**(2), 211–221 (2004)
9. Birglen, L., Gosselin, C.M.: Fuzzy enhanced control of an underactuated finger using tactile and position sensors. In: Proceeding IEEE International Conference on Robotics and Automation, Barcelona, Spain, April 2005, pp. 2320–2325 (2005)
10. Dollar, A.M., Howe, R.D.: The SDM hand as a prosthetic terminal device: a feasibility study. In: 2007 IEEE 10th International Conference on Rehabilitation Robotics, Noordwijk, Netherlands, June, pp. 978–983 (2007)
11. Carbone, G., Iannone, S., Ceccarelli, M.: Regulation and control of LARM Hand III. Robot. Comput. Integr. Manuf. **24**(2), 202–211 (2010)
12. Zhang, W., Che, D., Liu, H., et al.: Super under-actuated multi-fingered mechanical hand with modular self-adaptive gear-rack mechanism. Ind. Robot Int. J. **36**(3), 255–262 (2009)
13. Li, G., Li, B., Sun, J., et al.: The development of a directly self-adaptive robot hand with pulley-belt mechanism. Int. J. Precis. Eng. Manuf. **14**(8), 1361–1368 (2013)
14. Li, G., Liu, H., Zhang, W.: Development of multi-fingered robotic hand with coupled and directly self-adaptive grasp. Int. J. Humanoid Rob. **9**(4), 1–18 (2012). Article ID 1250034
15. Zhang, W., Zhao, D., Zhou, H., et al.: Two-DOF coupled and self-adaptive (COSA) finger: a novel under-actuated mechanism. Int. J. Humanoid Rob. **10**(2), 1–26 (2013)